Biol. Stud. 2013: 7(2); 5–14 • DOI: https://doi.org/10.30970/sbi.0702.277
www.http://publications.lnu.edu.ua/journals/index.php/biology

UDC 576:577

CONTRIBUTION OF PERFUSION IN DIFFUSION-WEIGHTED ^{1}H-MRI OF INTRAHEPATIC AND SUBCUTANEOUS HEPATOCELLULAR CARCINOMA IN RAT

A. M. Babsky[1,2], ***B. George***[1], ***V. P. Greniukh***[2], ***N. Bansal***[1]

[1] *Department of Radiology and Imaging Sciences, Indiana University, Indianapolis, IN, 46202, USA*

[2] *Ivan Franko National University of Lviv, 4, Hrushevskyi St., Lviv 79005, Ukraine*
e-mail: andriy10@yahoo.com

Hepatocellular carcinoma (HCC) and liver metastases are an increasing problem worldwide. Non-invasive methods for understanding of HCC growth mechanisms are highly desirable. A biexponential model for analysis of non-invasive diffusion-weighted ^{1}H magnetic resonance imaging (MRI) provides important information about neoplastic transformation in capillary liver tissue perfusion and water molecular diffusion. Fast and slow components of water apparent diffusion coefficient (ADC) were separated in the normal rat liver, intrahepatic, and subcutaneous HCCs. MRI was acquired with a Varian 9.4 T horizontal bore system. The fast component of ADC (ADC_{fast}), which contributes 38% to total signal in the intrahepatic HCC, was significantly lower compared to normal liver value, while the slow component of ADC did not differ in liver, intrahepatic, and subcutaneous HCCs. A decrease in ADC_{fast} may be caused by restricted perfusion in abnormal tumor microvessels. Thus, a reported earlier decrease in ADC in HCC compared to normal liver was mostly due to a decreased in tumor perfusion rather than a decrease in water diffusion. Subcutaneous HCC showed a very limited vasculature development, which makes the tumor perfusion extremely poor and hypoxic. Simultaneous monitoring of water ADC changes in orthotopic and subcutaneous HCCs may be useful, but a possibility of location-based physiological and metabolic differences must be recognized.

Keywords: hepatocellular carcinoma, ^{1}H-MRI, apparent diffusion coefficient, perfusion, tumor location.

INTRODUCTION

Hepatocellular carcinoma (HCC) and liver metastases from other tumors are an increasing problem worldwide due to the major risk factors of HCC growth, such as cirrhosis and hepatitis, which cause genetic changes that lead to neoplastic transformations [19]. Measurements of apparent diffusion coefficient of water (ADC) by diffusion-weighted ^{1}H magnetic resonance imaging (MRI) has potential values in characterizing hepatic pathological alterations, differentiating between malignant and benign tumors, and estimating of therapy efficacy [21, 23, 26]. As a quantitative parameter calculated

from diffusion-weighted ^{1}H MRI (DWI), water ADC may reflect not only diffusion that represents mostly the Brownian motion of the water molecules, but also perfusion in microvessels, particularly in tissues with a rich vasculature such as normal liver and intrahepatic HCC [10]. Previous studies showed that for low strength of the diffusion weighting (*b*-values < 100 s/mm^2) perfusion dominated diffusion by a factor of 10. However, by using high *b*-values (> 500 s/mm^2), the influence of perfusion is largely attenuated [5]. Water ADC in HCC, metastases, and hepatic angiomas are generally reported to be mostly higher than those of hepatic parenchyma, but lower ADC in the tumor tissue has been also detected [5]. In addition to molecular diffusion and tissue perfusion, *in vivo* ADC measurements can be sensitive to respiratory and cardiac motion [18]. In human studies the effects of respiratory motion can be significantly reduced by performing diffusion studies in a single breath hold with rapid imaging techniques (e.g. echo planar imaging) [9]. In animal studies, in order to avoid possible motion artifacts and/or to obtain high quality MRI, subcutaneous tumor models instead of orthotopic models are frequently used [4, 11, 14, 15, 20, 24, 27]. However, tumor location can have a dramatic impact on water ADC values due to variation in vascularity, cell packing, and intratumor temperature [6–8, 12]. The tumor microenvironment can also be significantly affecting by nearby host tissue influencing water ADC in the tumor. Therefore, ADC in subcutaneous and intrahepatic tumors can be different and may change in distinctive way with tumor growth. To our knowledge, simultaneous assessment of perfusion and diffusion in intrahepatic and subcutaneous HCCs has not been performed.

In this study, the perfusion (*b*-values = 0, 10, 20, 30, and 100 s/mm^2) and diffusion (*b*-values = 220, 350, 600, 1000, and 1600 s/mm^2) components of water ADC in rat liver, and intrahepatic and subcutaneous HCCs were compared. The objective of the study was to evaluate possible contribution of capillary tissue perfusion and water molecular diffusion in diffusion-weighted ^{1}H-MRI (DWI) of HCCs located intrahepatically and subcutaneously.

MATERIALS AND METHODS

Tumor model: All animal studies were approved by the Indiana University Institutional Animal Care and Use Committee. N1S1 cells (American Type Tissue Culture Collection, Bethesda, MD, USA), a rat Novikoff hepatoma cell line, was maintained as an exponentially growing suspension in Iscove modified Dulbecco's Medium (Sigma-Aldrich, St. Louis, MO, USA). Male Sprague-Dawley rats (Harlan, Indianapolis, IN, USA) approximately 12–13 weeks of age were anesthetized with isoflurane (2%) in medical air for tumor inoculation. To initiate the intrahepatic and subcutaneous tumors, 10^6 cells in 0.1 ml phosphate buffered saline solution were injected in the left lateral lobe of the liver and 10^7 cells were inoculated under the skin on the thigh, respectively. Each animal was imaged 21 (intrahepatic HCC) or 28 days (subcutaneous HCC) after injection of cells. Tumor volume was measured from T_2 ^{1}H images with *b*-value = 0 s/mm^2.

MRI experiments: All *in vivo* MRIs were acquired with a 9.4 Tesla, 31-cm horizontal bore system (Varian, Palo Alto, CA, USA). Animals were anesthetized with 1–1.5% isoflurane delivered in medical air at 1.0–1.5 L/min using a rat nose mask connected to a gas anesthesia machine (Vetland, Louisville, KY, USA). Warm air was blown through the magnet bore to maintain the temperature in the space surrounding the animal and the animal core body temperature at 26–28°C and 32–36°C, respectively. Respiration was monitored with a physiological monitoring and gating system (SA Instruments, Stony Brook, NY, USA) using a pneumatic pillow located under the animal's abdominal area.

^{1}H MRI: Water ADC of the HCCs and normal liver tissue was measured with a 63-mm birdcage coil. A multi-slice DWI sequence with the following imaging parameters was used: 1,100 ms repetition time, 21 ms echo time, 256×128 data points over a 80×80 field of view, 0.5 mm slice thickness, 1.5 mm slice gap, and b = 0, 10, 20, 30, 100, 220, 350, 600, 1000, and 1600 s/mm^2. In case of intrahepatic HCC respiratory gating was used to minimize the motion effect on water ADC. In addition, the animal respiration rate was brought to a relatively stable level (40±2 breaths/min) to minimize variation in repetition time by slightly adjusted the isoflurane anesthesia. Total data collection time for a set of DWI at the ten b values was ~23 min.

Data analysis and statistics: ^{1}H images were reconstructed by using the Image Browser software (Varian, Palo Alto, CA, USA). Tumor volume and average water ADC were determined over a three-dimensional volume of interest for each temporal measurement. PSI-PLOT software was used to analyze ADC_{fast} and ADC_{slow} components. DWI signal intensity (SI) versus b value data were fit to the following biexponential equation for normal liver and intrahepatic HCC: , where A_0 is signal intensity for a b= 0 s/mm^2, ADC_{fast} and ADC_{slow} are the fast and slow ADC component which are related to tissue perfusion and random molecular diffusion of water, respectively, and A_f is the relative contribution of ADC_{fast} which is related to the relative vascular volume or the fraction of fast moving ADC. A monoexponential equation was used for subcutaneous HCC.

All statistical data are presented as the mean ± standard error of mean (SEM) and represent the range across a cohort of animals. In figures 2, 4, and 6, the error bars show only one side of the symmetric values for clear visibility. Analysis of the data was performed using Student's t-test. A P value J 0.05 was used to define statistical significance.

RESULTS

Transaxial sections of DWI of the rat liver, intrahepatic and subcutaneous HCCs collected using ten b values are shown in Fig. 1. Both intrahepatic and subcutaneous HCCs are marked by T-arrows and liver is marked by L-arrow while reference containing 0.03% NaCl is marked by R- arrow. The images of the liver containing HCC was slightly blurred with b-values of 100-1600 s/mm^2 even though they were collected with respiratory gating, nevertheless, the ADC map showed only a fair motion effect in the liver region [1, 2]. DWI of subcutaneous HCC did not show any blurring (Fig. 1).

The mean DWI signal intensity vs. b-values in intrahepatic and subcutaneous HCCs, and nearby normal liver is shown in Fig. 2. In intrahepatic and subcutaneous HCCs, ^{1}H signal intensity with b = 0 s/mm^2 was almost 2 and 1.5 times higher, respectively, compared to normal liver (Fig. 2). In normal liver and intrahepatic HCC, the curves that describe the DWI signal intensity changes with different b-values were biexponential, reflecting significant contribution of the circulatory system. In subcutaneous HCC, the curve that describes the DWI signal intensity changes with different b-values was monoexponential, reflecting very poor development of the circulatory system (Fig. 2).

Table 1 presents the characteristics of fast and slow components of water ADC in the liver, intrahepatic and subcutaneous HCCs. A_f in the liver was 0.31, while the values of ADC_{fast} and ADC_{slow} were 20.2 and 0.70 mm^2/s, respectively. In the intrahepatic HCC, A_f was 0.38, while the value of ADC_{fast} was lower (9.35 mm^2/s, P = 0.05) and ADC_{slow} was similar (0.70 mm^2/s) compared to the healthy liver. In subcutaneous HCC model, ADC_{slow} (0.65 mm^2/s) did not differ compared to intrahepatic HCC and liver (Table 1). The diffusion coefficient of water in the reference was always 2.3±0.01×10^{-3} mm^2/s, as measured by using monoexponential curve or ADC map [2].

Table 1. **Fast and slow components of water ADC in rat liver, intrahepatic (IH) and subcutaneous (SC) HCC**

Таблиця 1. **Швидка та повільна компоненти коефіцієнта дифузії води у печінці, ортотопній (IH) і підшкірній (SC) гепатоклітинній карциномі щура**

Parameter	Liver	IH-HCC	SC-HCC
A_0	99 ± 7	193 ± 13*	163 ± 9*
A_f	0.31 ± 0.05	0.38 ± 0.05	0
ADC_{fast}	20.2 ± 5.3	9.35 ± 1.62*	–
ADC_{slow}	0.70 ± 0.08	0.70 ± 0.09	0.65 ± 0.02

Comment: * – $P \leq 0.05$ comparing to liver.

Примітка: * – $P \leq 0,05$ порівняно з печінкою.

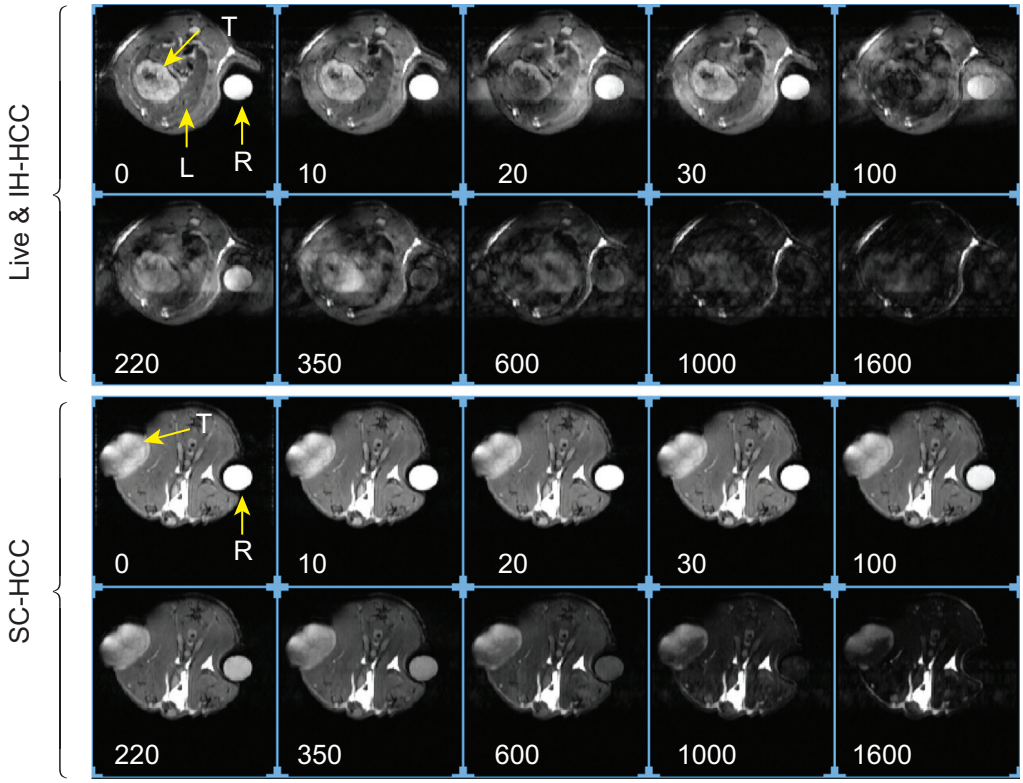

Fig. 1. Representative transaxial slices of diffusion-weighted ^{1}H MRI of the rat liver, intrahepatic (IH) and subcutaneous (SC) HCC with different *b* values. HCCs, liver and reference are marked by arrows T, L and R, respectively. *b*-values are in s/mm^2. The tube filled by 0.3 mM NaCl was used as a reference

Рис. 1. Типові зображення поперечних зрізів дифузійно-градієнтного ^{1}H-магнітного резонансу печінки щурів, ортотопної (IH) та підшкірної (SC) гепатоклітинної карциноми з різними значеннями *b*. Карциноми, нормальна печінка і стандарт позначені відповідно стрілками T, L і R. Значення *b* представлені в с/мм^2. Стандартом слугувала пробірка із 0,3 мМ NaCl

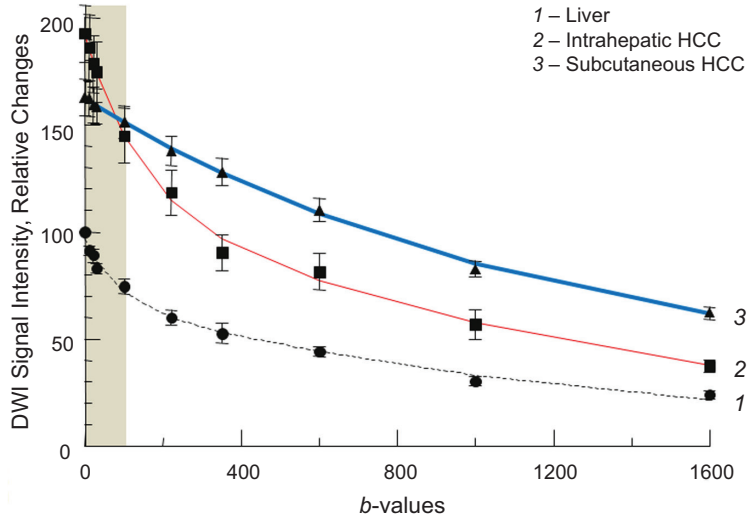

Fig. 2. Perfusion and diffusion component of ADC in rat liver, intrahepatic and subcutaneous HCCs (mean ± SEM, n = 8). The signal intensity in liver with b = 0 s/mm² is normalized to 100. Shading indicates the perfusion component area

Рис. 2. Перфузійний і дифузійний компоненти коефіцієнта дифузії води у печінці, ортотопній і підшкірній гепатоклітинній карциномах щурів (M ± m, n = 8). Інтенсивність сигналу в печінці з b = 0 с/мм² нормалізована до 100. Затінення вказує на ділянку перфузійної компоненти

Fig.3 shows selective X-ray angiography of the normal hepatic, intrahepatic HCC, and subcutaneous HCC vascularity when barium suspension was injected into the heart. The normal hepatic tissue has very well developed and structural vascular system (*1*). Intrahepatic HCC has less developed vasculature (*2*) compared to normal liver tissue but still is fine compared to other tumor tissue. Large subcutaneous HCC shows very limited vasculature development (*3*), which makes the tumor extremely unperfused and hypoxic.

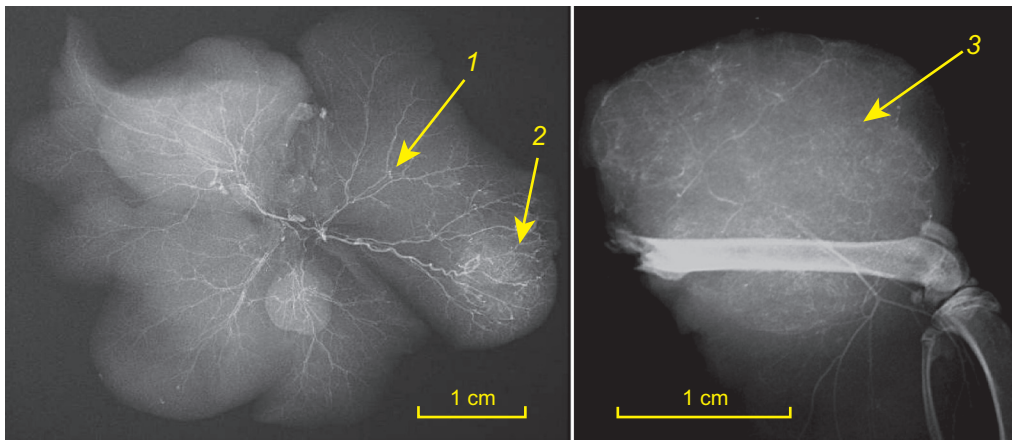

Fig. 3. Selective X-ray angiography of normal liver (*1*), intrahepatic HCC (*2*), and subcutaneous HCC (*3*). Barium suspension was injected into the heart by syringe

Рис. 3. Рентгенівська ангіографія нормальної печінки (1), ортотопної (2) та підшкірної гепатоклітинної карциноми (3). Суспензію барію було введено в серце за допомогою шприца

DISCUSSION

In this work, the perfusion and diffusion components of water ADC in the rat liver, intrahepatic and subcutaneous HCCs were compared to evaluate the possible contribution of capillary tissue perfusion in DWI of HCCs located orthotopically and under the skin. Water ADC measurements in HCC, metastases, and hepatic angiomas are usually higher than those of hepatic parenchyma [7]. A higher ADC in intrahepatic HCC compared to the nearby liver has also been reported in previous human studies [5, 11, 17, 25]. The common explanation of this effect invokes less differentiation of tumor cells and a net increase in the tumor relative extracellular space (ECS). Histology of intrahepatic HCC and liver after the last MRI experiment showed that relative ECS in the viable tumor regions was larger than in the healthy liver mostly due to reduction in cellular cytoplasm [2]. Furthermore, intrahepatic HCC contained areas of inflammation and necrosis with a large ECS in which water diffusion could be faster compared to the intracellular space [1, 16]. However, traditional DWI measurements include a contributory perfusion component, particularly in tissues with a rich vasculature such as intrahepatic HCC. The presented data show that ADC_{fast}, which contributes 38% to the total signal in intrahepatic HCC, is significantly lower compared to the normal liver value. This decrease may be caused by restricted perfusion in abnormal tumor microvessels. Thus, earlier reported decrease in ADC in HCC compared to normal liver when mono-exponential analysis of ADC maps has been used, was mostly due to perfusion decreased in tumor rather than a restriction in water diffusion [2, 3]. The X-ray angiography shows that normal hepatic tissue has superior vascular system while vascularity of HCC depends on the tumor location. Intrahepatic HCC possesses less developed vasculature then normal liver, but is still relatively rich compared to other tumor tissues [22]. Subcutaneous HCC shows very limited vasculature development, which makes the tumor perfusion extremely poor and hypoxic. DWI data support this conclusion not-showing ADC_{fast} component in HCC under the skin.

Respiratory motion may also contribute to ADC_{fast} because the motion artifact was clearly visible in liver bearing HCC. However, the motion did not affect ADC_{slow} which was similar to that of subcutaneous HCC which is insensitive to abdominal motion. Thus, in subcutaneous HCC, the earlier reported water ADC could be lower than the intrahepatic HCC due to small vascular space and very low perfusion. To further support this explanation, additional histology and immunohistochemistry experiments should be done.

Thus, simultaneous monitoring of water ADC changes in intrahepatic and subcutaneous HCCs may be useful, but the possibility of location-based physiological and metabolic differences must be recognized. Vascular architecture and its response to therapy not only vary among tumor types, but may differ between transplanted and spontaneous tumors [8]. These differences may lead to different altering in ADC to chemo-, radio-, or immunotherapy.

CONCLUSION

A biexponential model for analysis of non-invasive DWI provides important information about neoplastic transformation in capillary liver tissue perfusion and water molecular diffusion. Recognition of both perfusion and diffusion components of water ADC may be important for monitoring tumor growth and response to therapy of orthotopic and metastatic HCC.

ACKNOWLEDGEMENTS

The authors gratefully acknowledge Ms. Stacy Bennett for technical assistance and Dr. S. Greg Jennings for valuable discussion and editorial comments. This research was supported in part by NIH grant R01EB005964.

1. *Babsky A., Ju S., Bansal N.* Evaluation of tumor treatment response with diffusion-weighted MRI. In: Taouli B. (Ed.) **Extra-Cranial Application of Diffusion – Weighted MRI.** Cambridge: University Press, 2011: 172–197.
2. *Babsky A.M., Ju S., Bennett S. et al.* Effect of implantation site and growth of hepatocellular carcinoma on apparent diffusion coefficient of water and sodium MRI. **NMR in Biomedicine,** 2012; 25(2): 312–321.
3. *Babsky A.M., Ju S., George B.* et al. Predicting response to benzamide riboside chemotherapy in hepatocellular carcinoma using apparent diffusion coefficient of water. **Anticancer Research,** 2011; 31(6): 2045–2051.
4. *Babsky A.M., Zhang H., Hekmatyar S.K. et al.* Monitoring chemotherapeutic response in RIF-1 tumors by single-quantum and triple-quantum-filtered ^{23}Na MRI, ^{1}H diffusion-weighted MRI and PET imaging. **Magnetic Resonance Imaging**, 2007; 25(7): 1015–1023.
5. *Colagrande S., Carbone S.F., Carusi L.M.* et al. Magnetic resonance diffusion-weighted imaging: extraneurological applications. **Radiologia Medica**, 2006; 111(3): 392–419.
6. *Dave S., Vaupel P., Mueller-Kliesser P., Blendstrup K.* Temperature distribution in peripheral s.c. tumors in rats. In: *Overgaard J.* (Ed.) **Hyperthermia Oncology**. London: Taylor and Francis, 1984: 503–506.
7. *Falk P.* Differences in vascular pattern between the spontaneous and the transplanted C3H mouse mammary carcinoma. **European Journal of Cancer and Clinical Oncology**, 1982; 18(2): 155–165.
8. *Field S.B., Needham S., Burney I.A.* et al. Differences in vascular response between primary and transplanted tumours. **British Journal of Cancer**, 1991; 63(5): 723-726.
9. *Goshima S., Kanematsu M., Kondo H.* et al. Diffusion-weighted imaging of the liver: optimizing b value for the detection and characterization of benign and malignant hepatic lesions. **Magnetic Resonance Imaging**, 2008; 28(3): 691–697.
10. *Guan S., Zhao W.D., Zhou K.R.* et al. Assessment of hemodynamics in precancerous lesion of hepatocellular carcinoma: evaluation with MR perfusion. **World Journal of Gastroenterology,** 2007; 13(8): 1182–1186.
11. *Ichikawa T., Haradome H., Hachiya J.* et al. Diffusion-weighted MR imaging with a single-shot echoplanar sequence: detection and characterization of focal hepatic lesions. **American Journal of Roentgenology,** 1998; 170(2): 397–402.
12. *Jayasundar R., Honess D., Hall L.D., Bleehen N.M*. Simultaneous evaluation of the effects of RF hyperthermia on the intra- and extracellular tumor pH. **Magnetic Resonance in Medicine,** 2000; 43(1):1–8.
13. *Jennings D., Hatton B.N., Guo J.* et al. Early response of prostate carcinoma xenografts to docetaxel chemotherapy monitored with diffusion MRI. **Neoplasia**, 2002; 4(3): 255–262.
14. *Jordan B.F., Runquist M., Raghunand N.* et al. Dynamic contrast-enhanced and diffusion MRI show rapid and dramatic changes in tumor microenvironment in response to inhibition of HIF-1alpha using PX-478. **Neoplasia,** 2005; 7(5): 475–485.
15. *Lemaire L., Howe F.A., Rodrigues L.M., Griffiths J.R.* Assessment of induced rat mammary tumour response to chemotherapy using the apparent diffusion coefficient of tissue water as determined by diffusion-weighted ^{1}H-NMR spectroscopy *in vivo*. **Magnetic Resonance Materials in Physics, Biology and Medicine,** 1999; 8(1): 20–26.

16. *Morse D.L., Galons J.P., Payne C.M.* et al. MRI-measured water mobility increases in response to chemotherapy via multiple cell-death mechanisms. **NMR in Biomedicine**, 2007; 20(6): 602–614.
17. *Namimoto T., Yamashita Y., Sumi S.* et al. Focal liver masses: characterization with diffusion-weighted echo-planar MR imaging. **Radiology,** 1997; 204(3): 739–744.
18. *Padhani A., Liu G., Koh D.M.* et al. Diffusion-weighted magnetic resonance imaging as a cancer biomarker: consensus and recommendations. **Neoplasia,** 2009; 11(2): 102-125.
19. *Parkin D.M., Bray F., Ferlay J., Pisani P*. Estimating the world cancer burden: Globocan 2000. **International Journal of Cancer**, 2001; 94(2): 153–156.
20. *Seierstad T,. Folkvord S., Roe K.* et al. Early changes in apparent diffusion coefficient predict the quantitative antitumoral activity of capecitabine, oxaliplatin, and irradiation in HT29 xenografts in athymic nude mice. **Neoplasia,** 2007; 9(5): 392–400.
21. *Sun X., Wang H., Chen F.* et al. Diffusion-weighted MRI of hepatic tumor in rats: Comparison between *in vivo* and postmortem imaging acquisitions. **Magnetic Resonance Imaging,** 2009; 29(3): 621–628.
22. *Taouli B., Koh D.-M.* Diffusion-weighted MRI of the liver. In: Taouli B. (Ed.) **Extra-Cranial Application of Diffusion - Weighted MRI.** Cambridge: University Press, 2011: 18–31.
23. *Taouli B., Vilgrain V., Dumont E.* et al. Evaluation of liver diffusion isotropy and characterization of focal hepatic lesions with two single-shot echo-planar MR imaging sequences: prospective study in 66 patients. **Radiology**, 2003; 226(1): 71–78.
24. *Thoeny H.C., De Keyzer F., Chen F.* et al. Diffusion-weighted magnetic resonance imaging allows noninvasive in vivo monitoring of the effects of combretastatin a-4 phosphate after repeated administration. **Neoplasia,** 2005; 7(8): 779–787.
25. *Yamada I., Aung W., Himeno Y.* et al. Diffusion coefficients in abdominal organs and hepatic lesions: evaluation with intravoxel incoherent motion echo-planar MR imaging. **Radiology,** 1999; 210(3): 617–623.
26. *Yuan Y.H., Xiao E.H., Liu J.B.* et al. Characteristics of liver on magnetic resonance diffusion-weighted imaging: dynamic and image pathological investigation in rabbit liver VX-2 tumor model. **World Journal of Gastroenterology,** 2008; 14(25): 3997–4004.
27. *Zhao M., Pipe J.G., Bonnett J., Evelhoch J.L.* Early detection of treatment response by diffusion-weighted ^{1}H-NMR spectroscopy in a murine tumour *in vivo*. **British Journal of Cancer**, 1996; 73(1): 61–64.

ВКЛАД ПЕРФУЗІЙНИХ ПРОЦЕСІВ У ДИФУЗІЙНО-ГРАДІЄНТНИХ ^{1}Н-ЗОБРАЖЕННЯХ МАГНІТНО-РЕЗОНАНСНОЇ ТОМОГРАФІЇ ОРТОТОПНОЇ ТА ПІДШКІРНОЇ ГЕПАТОКЛІТИННОЇ КАРЦИНОМИ У ЩУРІВ

***А. М. Бабський*[1,2], *Б. Джордж*[1], *В. П. Гренюх*[2], *Н.Банзал*[1]**

[1] *Індіанський університет, Індіанаполіс, США*

[2] *Львівський національний університет імені Івана Франка*
вул. Грушевського, 4, Львів 79005, Україна
e-mail: andriy10@yahoo.com

Неінвазивні методи дослідження карциноми печінки та ракових метастазів у цьому органі залишаються надзвичайно актуальними для вивчення механізмів канцерогенних перетворень, ранньої діагностики й оцінки ефективності хіміо- і радіотерапії. Діекспоненційна модель аналізу дифузійно-градієнтних ^{1}Н-зображень

магнітно-резонансної томографії (МРТ) гепатоклітинної карциноми (ГКК) дає змогу отримати важливу інформацію про канцерогенні зміни перфузії у капілярах печінки та дифузії молекул води в цій тканині. Швидка (перфузійна) і повільна (дифузійна) складові коефіцієнта дифузії води (КДВ) були розмежовані при аналізі КДВ у нормальній печінці, ортотопній і підшкірній ГКК. Зображення МРТ реєстрували на горизонтальній установці фірми Varian за умов зовнішнього магнітного поля значенням 9,4 Тл. У ГКК, локалізованій у печінці, швидка складова КДВ ($КДВ_{шв}$), яка становить 38% загального сигналу пухлини, була нижчою порівняно із нормальною печінкою, тоді як повільна складова КДВ не відрізнялась у нормальній печінці та ГКК, локалізованих у печінці та під шкірою. Зниження $КДВ_{шв}$ могло бути викликане обмеженням перфузії у невнормованій системі капілярів у пухлині. Таким чином, опубліковані раніше дані (на підставі аналізу мап КДВ чи за допомогою моноекспоненційної моделі обрахунку) про зниження цього показника за умов канцерогенезу були обумовлені в основному сповільненням перфузійних процесів. Одночасний неінвазивний моніторинг КДВ в ортотопній і підшкірній ГКК можна використовувати з урахуванням фізіологічних і метаболічних особливостей канцерогенезу різної локалізації.

Ключові слова: карцинома, печінка, МРТ, перфузія, дифузія води.

ПЕРФУЗИОННАЯ СОСТАВЛЯЮЩАЯ В ДИФФУЗИОННО-ГРАДИЕНТНЫХ ^{1}Н-ИЗОБРАЖЕНИЯХ МАГНИТНО-РЕЗОНАНСНОЙ ТОМОГРАФИИ ОРТОТОПНОЙ И ПОДКОЖНОЙ ГЕПАТОЦЕЛЛЮЛЯРНОЙ КАРЦИНОМЫ КРЫСЫ

А. М. Бабский[1,2]***, Б. Джордж***[1]***, В. П. Гренюх***[2]***, Н. Банзал***[1]

[1] *Индианский университет, Индианаполис, США*

[2]*Львовский национальный университет имени Ивана Франко*
ул. Грушевского, 4, Львов 79005, Украина
e-mail: andriy10@yahoo.com

Неинвазивные методы исследований карциномы печени и раковых метастаз в этом органе имеют хорошие перспективы использования в исследованиях механизмов канцерогенных преобразований, при ранней диагностике и оценке эффективности химио- и радиотерапии. Биэкспоненциальная модель анализа диффузионно-градиентных ^{1}Н-изображений ядерного магнитного резонанса (ЯМР) гепатоцеллюлярной карциномы (ГЦК) позволяет получать важную информацию о канцерогенных изменениях перфузии в капиллярах печени и диффузии молекул воды в этой ткани. Быстрая (перфузионная) и медленная (диффузионная) составляющие коэффициента диффузии воды (КДВ) были разделены при анализе КДВ в нормальной печени, ортотопной и подкожной ГЦК. Изображения ЯМР регистрировали с помощью горизонтальной установки фирмы Varian при силе внешнего магнитного поля 9,4 Тл. У ГЦК, локализированной в печени, быстрая компонента КДВ ($КДВ_{б}$), которая составляет 38% общего сигнала опухоли, была ниже в сравнении с нормальной печенью, тогда как медленная составляющая не отличалась в нормальной печени и ГЦК, локализованных ортотопно и подкожно. Снижение $КДВ_{б}$ могло быть вызвано снижением перфузии

в ненормированной системе капилляров опухоли. В ГЦК, локализованной в печени, быстрая составляющая КДВ была ниже в сравнении с нормальной печенью, в то время как медленная составляющая КДВ не отличалась в нормальной печени и ГЦК, локализованных и в печени, и под кожей. Таким образом, опубликованные ранее данные (на основании карт КДВ или с помощью моноэкспоненциальной модели анализа) о снижении этого показателя в условиях канцерогенеза были обусловлены в основном снижением интенсивности перфузионных процессов. Одновременный неинвазивный мониторинг КДВ в ортотопной и подкожной ГЦК можно использовать с учетом физиологических и метаболических особенностей канцерогенеза различной локализации.

Ключевые слова: карцинома, печень, ЯМР, перфузия, диффузия воды.

Одержано: 07.03.2013